A NEW NON-INDUCTIVE THUNDERSTORM ELECTRIFICATION SCHEME IN RAMS ATMOSPHERIC MODEL

A. Brandiyska[1,2], R. Mitzeva[2], B. Tsenova[3]

[1]Geophysical Institute, ul.Acad.G.Bonchev, bl3, Sofia1113, Bulgaria, e-mail: imdnme@gmail.com
[2]Sofia University, Faculty of Physics, 5 blvd. J. Bourchier, Sofia1164, Bulgaria, e-mail: rumypm@abv.bg
[3]National Institute of Meteorology and Hydrology, 66 Tzarigradsko Chaousee, Sofia1784, Bulgaria, e-mail: boryana.tsenova@abv.bg

Abstract. A new scheme of non-inductive thunderstorm electrification is developed, imbedded in the bulk microphysical scheme of RAMS v.6.0. The charge separation mechanisms use the rime accretion rate (RAR) approach (Brooks et al., 1997) and are based on the laboratory experiments of Takahashi (1978) and Saunders and colleagues (Saunders et al., 1991). A new type of hybrid scheme is tested, based on the assumption that the laboratory experiments of Saunders et al. (1991) (one-chamber) represent the charging in regions with weak mixing, while the experiments of Takahashi (1978) (two-chambers) represent the charging in regions with strong mixing. Numerical simulations of a typical thundercloud (CCOPE, 19 July 1981) indicate that the proposed hybrid scheme is capable to reproduce the basic charge structure of the storm in general agreement with observations.

Key words: modeling, thunderstorm, electricity, non-inductive charging

Introduction

Modeling of cloud electricity is an extremely challenging scientific problem for at least two reasons. First, thunderstorm models include processes of different scales – from macrophysical (km) to microphysical (nm), so the microphysical processes are parameterized and this leads to inevitable model uncertainty. Second, laboratory experiments on charge separation show controversial results for the sign and magnitude of the transferred charge. On the other hand, in-situ measurements of cloud microphysics and electricity, needed for proper verification of the model results, are available only for a few cases. Therefore, model simulations of thunderstorm electricity are still to a great extent

unreliable, but nevertheless they play a very important role in order to gain better insight into the interaction of different processes involved in the evolution of an electrified thunderstorm (MacGorman and Rust 1998). Cloud models, including atmospheric dynamics, misrophysics and electricity are the best tools for testing the validity of various electrification mechanisms.

In the scientific community it is accepted that the non-inductive charging mechanism plays the major role for thunderstorm electrification. Charge is generated (independently of external electric fields) during elastic collision between riming graupel and ice crystals in the presence of supercooled cloud droplets. The non-inductive charging mechanism was investigated in a number of experimental studies (Takahashi 1978; Jayaratne et al., 1983; Saunders et al., 1991; Saunders et al., 2004; Takahashi, 1999). The sign and the magnitude of the non-inductive charge transfer for a single collision depends on cloud temperature and cloud effective water content and is determined by the ability of graupel to capture supercooled water droplets. However, the experiments show contradictory results for the exact position of that line and the magnitude of the transferred charge. One possible explanation for the major differences between the experiments can be seen in the conditions in which the ice crystals were grown (Pereyra et al., 2000; Saunders et al., 2004). In the experiment of Takahashi from 1978 the crystals were grown in a separate volume and introduced to the droplet cloud on its way to the riming target, while in the Saunders and colleagues' experiment from 1991 the crystals were grown inside the droplet cloud, allowing them to achieve thermodynamical equilibrium with the water vapor. The two approaches are known as mixed cloud method (two chambers experiment) and single cloud method (one chamber experiment) and represent different thermodynamical conditions, that can be observed in different clouds or different parts of the same cloud (Pereyra et al., 2000) The one-cloud method represents conditions in which there is thermodynamical equilibrium between the particles and the environment, i.e. it is more appropriate to be used for the parameterization of charge transfer between graupel and ice crystals in the updraft while the second one is more representative for regions, where there is mixing between volumes of air having different history (Saunders et al., 2004; Mansell et al., 2005).

Brooks et al. (1997) suggested that a 'Rime Accretion Rate' (RAR) approach, which includes the effect of the relative velocity V of the interacting particles, is more appropriate than simply using the effective water (EW) to determine charge dependence on cloud conditions. They proposed modifications of the equations in Saunders et al. (1991) for the separated charge to be presented as a function of cloud temperature and RAR. Similar modifications can be easily performed on the equations proposed in Tsenova and Mitzeva (2009) for the dataset obtained by Takahashi (1978).

Our study continues the efforts of previous authors like Barthe et al. (2005) and Altaratz et al. (2005) to develop an electric scheme, coupled to a 3D mesoscale model. The new scheme is based on the same two sets of experimental data like all previous parameterizations, but includes some new physically based features, namely: 1) replacing EW with RAR for the calculation of separated charge and 2) adding a new type of hybrid scheme, based on the gradient of the vertical velocity.

The aim of the present study is to test the performance of the scheme by simulating a well-documented thunderstorm case (CCOPE 19 July 1981) and comparing

the model results to measurements. This test case will also help us choose the most appropriate threshold for the gradient of vertical velocity in the hybrid parameterization.

CCOPE'81 Case Study

The CCOPE 19 July 1981 case study, a small isolated mid-latitude thunderstorm which developed in southeastern Montana, is often used for validation of storm electrification models, because it is among the best documented ones. Instrumented aircraft and radar data were used to investigate the microphysical, electrical, and dynamic evolution of the cloud. The measurements are presented in Gardiner et al. (1985) and Dye et al. (1986).

The measured cloud base height was 3.8 km above sea level (ASL), corresponding to 3.0 km above ground level (AGL), maximum cloud top – 10.5 ASL, maximum velocity – 10-15 $m.s^{-1}$, maximum LWC – 2.5 $g.m^{-3}$. The first graupel particles were formed at an altitude between 6.5 и 7.5 km ASL.

Negative charge accumulation was observed at 16:30 MDT near the 7 km (−20°C) level, associated with the high reflectivity region. Between 16:32-16:36 MDT lots of negatively charged graupel particles were observed by the Aerocommander aircraft at 4.5 km associated with precipitation falling towards the ground (Dye et al., 1986). The extremum values of particle charge, measured in the 5-6 km ASL layer were +1.4 $nC.m^{-3}$ and –0.5 $nC.m^{-3}$. According to Dye et al. (1986), the cloud charge structure was a positive dipole (positive charge over negative) and the main positive charge was carried by pristine ice, snow and aggregates, while the main negative charge was carried by graupel. The peak in the electrical development of the cloud was at 16:37 MDT when an intracloud discharge was detected.

There are several previous modeling studies investigating the electrification of the same storm, using a 1D and 2D models (Norville, 1991; Brooks et al., 1997; Helsdon et al., 2001), where general comparison with observations of space and time electrical properties was made. Helsdon et al. (2001) concludes that both of the non-inductive (NI) schemes, based on Takahashi (1978) and Saunders et al. (1991) are capable of producing electrification that approaches thunderstorm levels. The NI mechanism, based on Takahashi's work, developed a positive dipole (positive charge above negative) and realistic electric fields, while the transferred charge based on the work of Saunders and colleagues had to be reduced in magnitude to produce electrification that is consistent with the observations. They also noticed that the Saunders scheme produced an initially inverted dipole (negative charge above positive) which resolves into a positive dipole later in the simulation.

The RAMS 6.0 electrical parametrization

The model used in the present study is RAMS (Regional Atmospheric Modeling System) v.6.0, which is developed by Colorado State University and is widely used as a research tool for numerical studies of thunderstorms (see Pielke et al., 1992; Cotton et al.,

2003). RAMS is a 3-dimensional non-hydrostatic cloud resolving atmospheric model. It includes equations and parameterizations for a wide range of physical processes: advection, diffusion, turbulence, radiation, large-scale precipitation, microphysics. Spatial resolution can vary from hundreds of meters to hundreds of kilometers and time step can be fixed or varying.

The two-moment bulk microphysical scheme in RAMS predicts both mass mixing ratio and number concentration of hydrometeor species thus allowing the mean diameter to evolve (Meyers et al., 1997). In the model, seven species of hydrometeors are categorized: cloud droplets, rain, pristine ice, snow, aggregates, graupel and hail. The cloud droplet and other types of hydrometeors spectra are approximated by a gamma function with fixed shape (Walko et al., 1995).

The version of RAMS v.4.4 with electricity, presented in Altaratz et al. (2005), was adapted for RAMS 6.0 and used as a reference frame for the transfer of charge between microphysical categories in the new scheme. However, the new electrification scheme is completely rewritten and there are significant differences in the way charge is calculated.

The electrification parameterization is imbedded inside the RAMS v.6.0 microphysical scheme. It calculates charge separation due to elastic collisions between big riming graupel particles and small ice crystals (pristine ice). There is no charge separation at temperatures above 0 □C.

The present scheme includes the parameterization of Brooks et al. (1997) (denoted with BR) and the parameterization based on the equations for Takahashi (1978) presented in Tsenova and Mitzeva (2009), with the charge calculated depending on RAR (denoted with T78_eq_RAR). In the present paper a new type of hybrid scheme is included, based on the concept that Saunders et al. (1991) laboratory experiment should be used where the particles have come to a steady growth state in their environment, and the Takahashi (1978) laboratory experiment – for simulations of situations with slow-growing ice crystals in a low-supersaturated environment entrained into a region of high supersaturation. Thus, the hybrid scheme uses one of the two parameterizations mentioned above — Brooks et al. (1997) and a new RAR based parameterization for Takahashi (1978) (see the equations in the Appendix). The choice of which parameterization to use depends on the relative vertical velocity of air in adjacent grid cells (i.e. the horizontal gradient of the vertical velocity), which is used as a measure for the intensity of the mixing. If the gradient is grater than a pre-defined threshold, we assume that the mixing is strong and the particles are not in equilibrium with the environment, so the scheme based on Tsenova and Mitzeva (2009), is used. If the gradient is smaller than the threshold, the parameterization based on Brooks et al. (1997), is used. In the present paper two different thresholds (2 and 5 $m.s^{-1}.km^{-1}$) are examined and the respective parameterizations are denoted with Hyb2 and Hyb5.

The charge transferred per collision event depends on the rime accretion rate - $RAR = EW * V$, where V is the mean relative velocity between the interacting categories and EW is the effective water content, which is calculated in the following way:

$$EW = (eff_9 \cdot r_c + eff_1 \cdot r_r) \cdot 1000 \cdot \rho_0 \qquad (1)$$

where r_c – cloud water mixing ratio; r_r – rain water mixing ratio; ρ_0 – air density;

eff_9 – collection efficiency between graupel and cloud droplets, which increases when the

mean mass of cloud droplets increases; eff_1 – collection efficiency between graupel and rain drops.

The charge transferred for one collision is calculated in the following way (Saunders et al., 1991):

$$\delta q = B \cdot (D_x)^{\alpha} \cdot \left| V_x(D_x) - V_y(D_y) \right|^{\beta} \cdot q_{\exp} \qquad (2)$$

where $q_{\exp}$ – experimental value for the separated charge; D_x – mean diameter of pristine ice; D_y – mean diameter of graupel,; $V_x(D_x) - V_y(D_y)$ –relative velocity of the colliding particles; B, α and β – constants, the values of which are given in Table 1. The table is taken from Tsenova and Mitzeva (2009).

The charge per separation is limited between -100 and 100 fC for the parameterizations based on Takahashi (1978) and between -200 and 500 fC for the parameterizations based on Saunders et al. (1991).

Table 1 Values of the constants α, β and B, depending on crystal size (D_x) and the sign of the charge. The values of B depend on the choice of parameterization (based on Saunders or Takahashi - B_{SKM} or B_{T78}). This table is taken from Tsenova and Mitzeva (2009).

Charge sign	Crystal size [μm]	α	β	B_{SKM}	B_{T78}
+Q	<155	3.76	2.5	4.9×10^{13}	6.1×10^{12}
+Q	155-452	1.9	2.5	4×10^{6}	5×10^{5}
+Q	>452	0.44	2.5	52.8	6.5
-Q	<253	2.54	2.8	5.24×10^{8}	4.3×10^{7}
-Q	>253	0.5	2.8	24	2

The rate of charge buildup due to collisions between two categories of hydrometeors (x for graupel and y for pristine ice) is:

$$\frac{dQ_x}{dt} = -\frac{dQ_y}{dt} = \qquad (3)$$
$$= \frac{\pi}{4} \cdot \iint (D_x + D_y)^2 \cdot \left| V_x(D_x) - V_y(D_y) \right| \cdot \varepsilon(x,y) \cdot N_x(D_x) \cdot N_y(D_y) \cdot \delta q \cdot dD_x \cdot dD_y$$

where D_x and D_y – diameters for categories x and y (for the respective bin); $V_x(D_x)$ and $V_y(D_y)$ – fall speeds for categories x and y; $\varepsilon(x,y)$ – separation efficiency (equal to 1.0 minus collection efficiency); N_x and N_y – number of particles with diameters, respectively, D_x and D_y ; δq – charge transferred for one collision

The integral for the rate of charge buildup is calculated numerically over all particle diameters from 0 to $10\,D_{x,y}$, split into 50 bins of width 0.2 $D_{x,y}$ for both categories. This is done in the most simple way:

$$I = \sum_{i=1}^{50}\sum_{j=1}^{50} F(D_{xi}, D_{yj}) \cdot dD_x \cdot dD_y \quad (4)$$

where $dD_x = 0.2 \cdot D_x$, $dD_y = 0.2 \cdot D_y$; $D_{xi} = i \cdot 0.2 \cdot D_x + 0.1 \cdot D_x$ and $D_{yj} = j \cdot 0.2 \cdot D_y + 0.1 \cdot D_y$ are the diameters for bin (i,j); $F(D_{xi}, D_{yj})$ is the value of the sub-integral function, with the values of all variables, calculated for the respective bins.

In addition to calculating charge separation, the scheme tracks the charge, carried by each of the 7 classes of hydrometeors in the microphysical scheme. The charge, created due to separations, is added to the existing charge for every grid cell and every category. There is a continuous transfer of mass between categories in the course of the cloud evolution, which is due to phase transitions, coalescence, shedding or other processes, and along with the transfer of mass the same portion of charge is also transferred. The transfer of mass due to sedimentation is also applied to charge.

For the calculation of the electric potential, a 3D Poisson equation is solved. In RAMS 4.4 this was done offline by using an external subroutine developed by Numerical Algorithms Group (NAG). In the present scheme we use a different approach for solving the Poisson equation, suitable for levels with varying thickness, but having lower computational efficiency – Liebman's 7-point iteration method. The boundary conditions are set to fair weather potential like in Altaraz et al. (2005). The critical electric field for lightning initiation is calculated like in Mansell et al. (2005), following Marshall et al. (1995):

$$E_{crit} = 201.7 * \exp(-z / 8.4) \quad (5)$$

where E is in kV/m and z is altitude AGL in km.

The calculations are carried out until the first lightning.

Model overview and set-up of the experiment

The model parameters used in the present study are shown in Table 2.

Table 2 Model parameters setup for the numerical simulations.

Parameter	Value
Horizontal resolution	64 km, 16 km, 4 km, 1 km
Vertical resolution at z=0m	30m
Vertical resolution above z=2000m	300m
Time step	90s, 30s, 15s, 5s
CCN number	$0.7*10^9$ #.m^{-3}
Gamma shape parameter, all species	2.0

The model domain covers the area of Miles City, USA with center point latitude/longitude of 46.6/-105.6. There are 4 nested domains with resolution 64, 16, 4, 1 km and size, respectively: 50x50, 50x50, 50x50, 74x74 points. The vertical coordinate is terrain-following sigma coordinate with level thickness ΔZ increasing from 30 m at ground level to 300 m in the free troposphere with a stretch ratio of 1.25. Initial and boundary

conditions are taken from the NCEP (US National Centers for Environmental Prediction) FNL global dataset with 1°x1° resolution. The appropriate physical options are selected, according to the RAMS Technical Manual (2010). The electric charge, carried by the 7 types of hydrometeors, is calculated in the innermost domain and the electric field is calculated every 3 min. The simulations are carried for the period 12:00 – 18:00 MDT with an automatically calculated time-step.

Results and discussion

Non-electrical aspects

A detailed discussion on the thunderstorm microphysical development can be found in previous studies, like Gardiner et al. (1985), Dye et al. (1986), Helsdon and Farley (1987). In the present paper we do not aim to reproduce exactly the same storm. For our purpose it is sufficient to reproduce the basic microphysical and electrical processes, that occurred in the cloud, so that the evolution of the simulated liquid water and ice species is similar to the observed ones from a qualitative point of view and their values are reasonable.

Convection in the innermost domain starts to develop after 16:00MDT, with cloud base of 2.3-2.6 km ASL. A total of 4 clouds develop which are shown on Fig. 1 and denoted with numbers 0, 1, 2 and 3 in the order of their appearance.

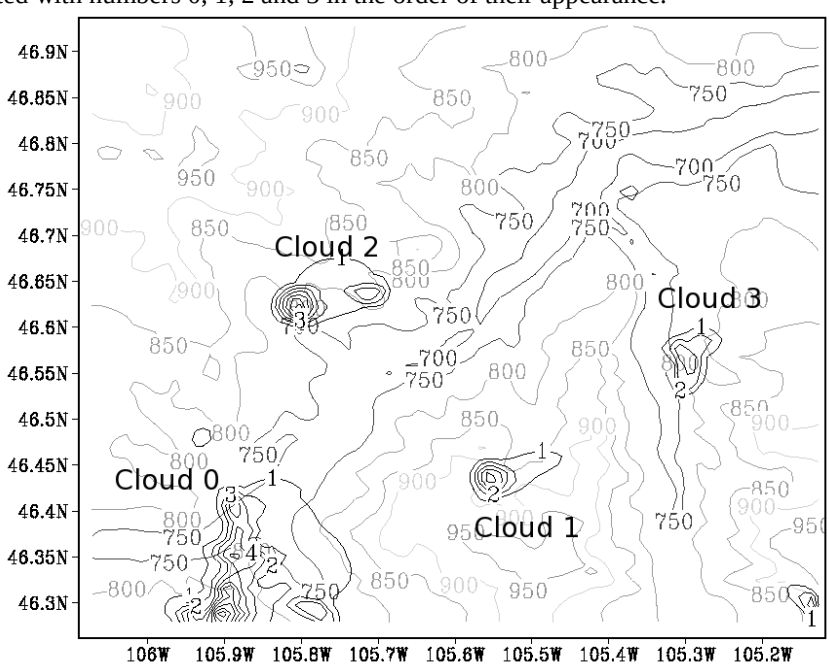

Fig. 1. Topography of the innermost domain (gray) and location of the three clouds (maximum liquid+ice content [g.m^{-3}] for 17:00MDT; black)

In this study we will not examine Cloud 0, because it is substantially larger and more intensive than the real storm (the cloud is more than 15km in diameter and the maximum value of the vertical velocity is W_{max}= 48 m.s^{-1}).

The first graupel particles in the real cloud are formed at an altitude between 6.5 и 7.5 km ASL, which corresponds to 5.8-6.8 km AGL. In the model simulations the first graupel particles form, respectively, at: 16:42, 5.8 km AGL for Cloud 1; at 16:45, 5.5 km AGL for Cloud 2; at 16:54, 6.1 km AGL for Cloud 3. Afterwards, there is a rapid growth phase in both the observations (Dye et al., 1986) and the simulations (not shown here), during which the liquid and ice particles grow and precipitation starts to form.

The results for the maximum values of the microphysical characteristics in the clouds are shown in Table 3.

Table 3 Maximum values of: vertical velocity W (m.s^{-1}); the content (in g.m^{-3}) of cloud water (cloud), total water (cloud+rain), total ice crystals (pristine+snow+aggregates), dense ice (graupel+hail) and total condensate (water+ice); precipitation intensity (mm/h) and accumulated precipitation (mm)

	W	Cloud water	Total water	Total ice crystals	Dense ice	Total condensate	Precipitation intensity	Accumulated precipitation
Cloud 1	30	2.7	6.5	0.9	5.0	7.0	65	13
Cloud 2	35	3.0	9.0	0.9	7.0	10.0	90	20
Cloud 3	27	3.0	6.5	1.0	4.5	8.0	70	14

The radar measurements show that the storm produced a moderate shower, which probably contained some hail (Dye et al., 1986). In the model simulations there is also a shower and in Cloud 1 the precipitation contains a small amount of hail, which is in general agreement with observations.

Considering the maximum vertical velocity (measured 15 m.s^{-1}, but outside the main core; simulated — 27-35 m.s^{-1}), the cloud top height (measured — 9.7 km AGL, simulated — 12 km AGL) and the maximum liquid water content (LWC) (measured — 2.5 g.m^{-3}, which is also outside the main core; simulated — 6.5-9 g.m^{-3}), we can conclude that all 3 clouds are more intensive than the real storm.

However, despite the qualitative differences between the simulated and the observed clouds, the simulation is quantitatively satisfying.

Electrical aspects

All 3 simulated clouds are more intensive than the real storm, but the evolution of the water and ice is similar, so we can expect that their electric structure would be similar to the structure of the real storm.

The temporal evolution of the charge density in clouds 1, 2 and 3 can be seen on Fig. 2, 3 and 4. Between 16:51 and 17:09 MDT all schemes produce charge density of reasonable magnitudes (the minimum values of total charge density are between -0.5 and -1.1 nC.m^{-3} and the maximum – between +0.6 and +1.6 nC.m^{-3}).

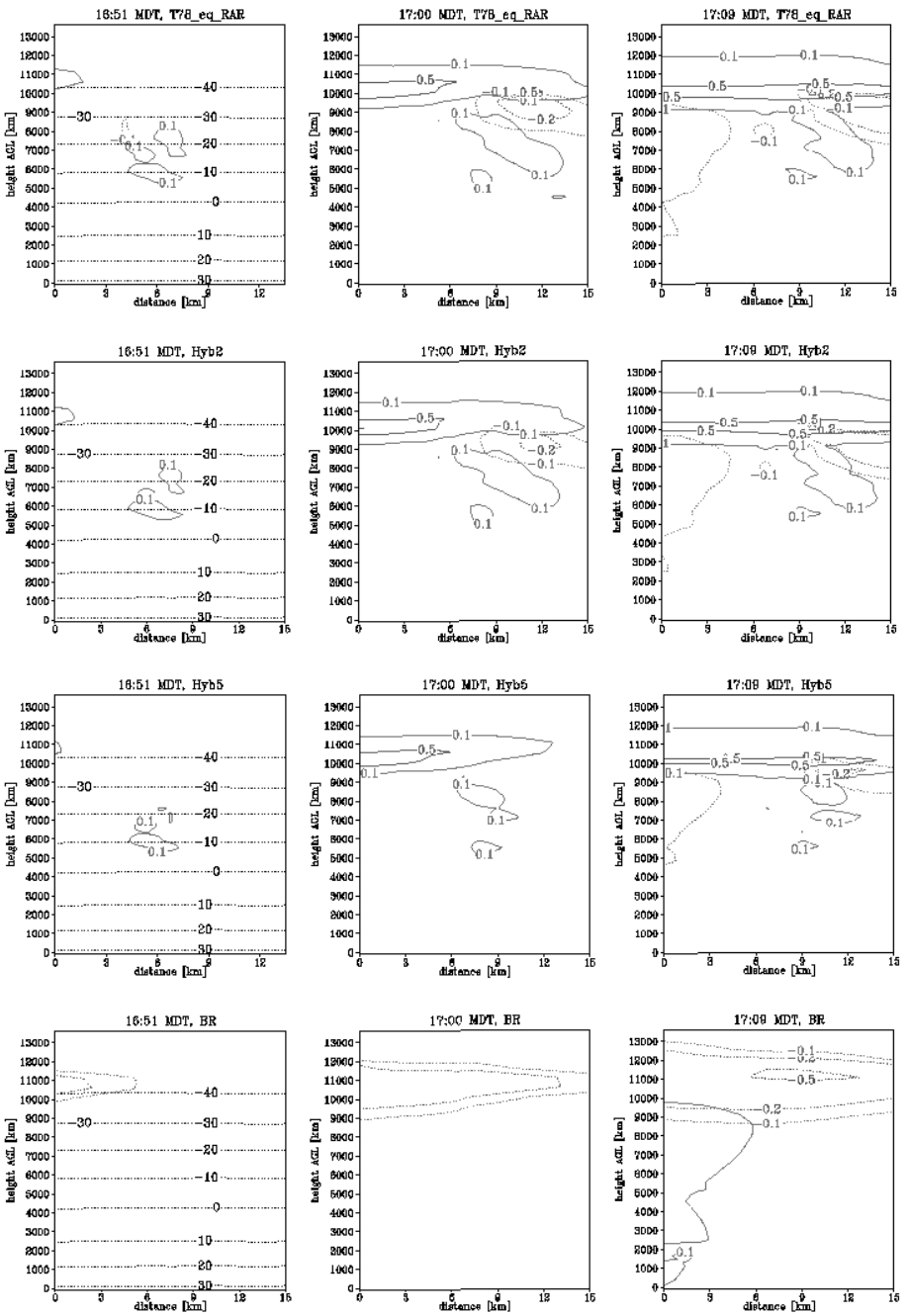

Fig. 2. Time evolution of the minimum (dotted) and maximum (solid) charge density (nC.m^{-3}), seen in NW direction for schemes T78_eq_RAR, Hyb2, Hyb5 and BR, Cloud 1

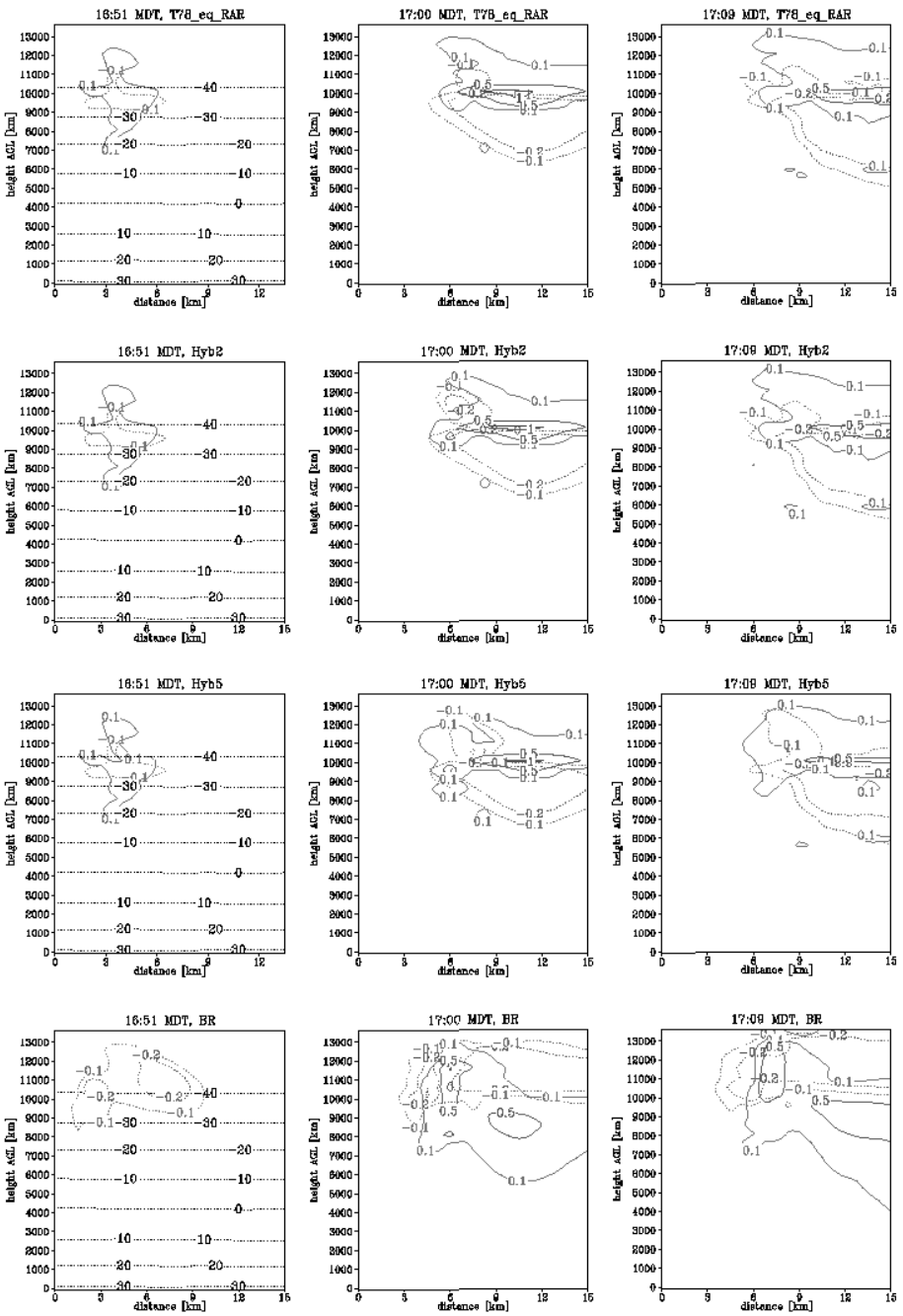

Fig. 3. Time evolution of the minimum (dotted) and maximum (solid) charge density (nC.m^{-3}), seen in NW direction for schemes T78_eq_RAR, Hyb2, Hyb5 and BR, Cloud 2

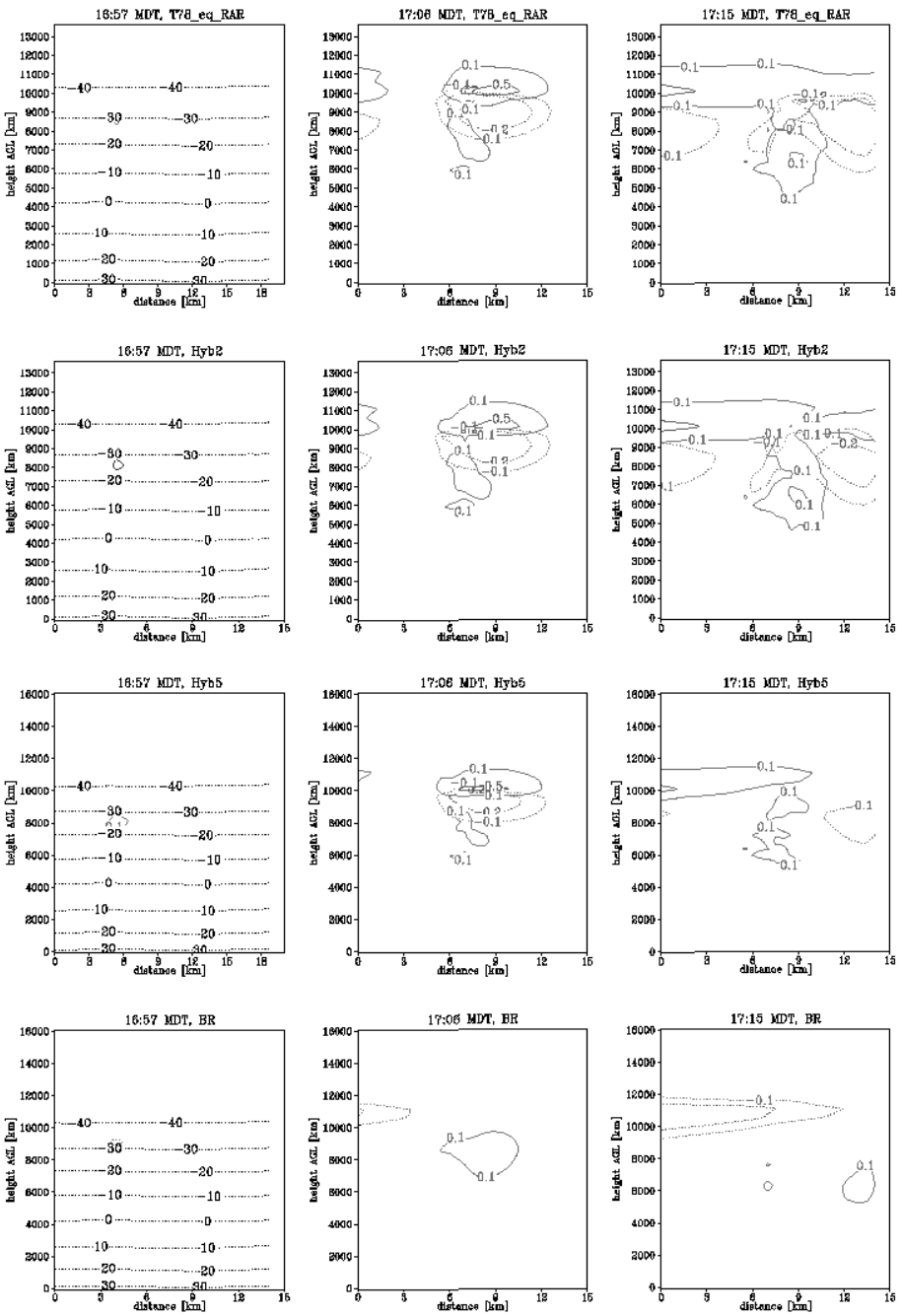

Fig. 4. Time evolution of the minimum (dotted) and maximum (solid) charge density (nC.m^{-3}), seen in NW direction for schemes T78_eq_RAR, Hyb2, Hyb5 and BR, Cloud 3

From the figures it can be seen, that the schemes T78_eq_RAR, Hyb2 and Hyb5 produce a positive dipole or tripole, as seen in the two right panels, while the BR scheme produces a monopole or a negative dipole. The positive dipole structure is more common (MacGorman and Rust, 1998) than the negative dipole and is in agreement with the observations (Dye et al., 1986). The lower positively charged region, which can be seen on the figures, is also common in thunderstorms (MacGorman and Rust, 1998) and there is evidence for the presence of such a positive charge in the CCOPE'81 cloud — the maximum values of the measured positive charge density in the 5-6 km ASL (4-5 km AGL) layer (just below the main negative charge) are +1.4 $nC.m^{-3}$ (Dye et al., 1986).

According to Dye et al. (1986), the main positive charge was carried by pristine ice, snow and aggregates, while the main negative charge was carried by graupel and hail. The simulated maximum and minimum (in space and time) values of the total charge density and the charge density carried by different types of hydrometeors are shown in Tables 4 and 5. Table 4 shows both clouds 1 and 2, because their values are identical. From the tables it can be seen, that BR and Hyb5 schemes produce large positive charge of graupel and hail and large negative charge of pristine, snow и aggregates. These results are not in agreement with the measurements. On the other hand, the schemes T78_eq_RAR and Hyb2 produce reasonable values that agree with the observations.

Table 4 Maximum in space and time simulated charge densities ($nC.m^{-3}$) for the schemes T78_eq_RAR, BR and the hybrid schemes with different values of the threshold (2 and 5 $m.s^{-1}.km^{-1}$ - Hyb2 and Hyb5). Cloud 1 and Cloud 2

	Max total negative	Max negative (p+s+a)	Max negative (g+h)	Max total positive	Max positive (p+s+a)	Max positive (g+h)
T78_eq_RAR	-0.5	-0.6	-1.0	0.6	1.2	0.7
Hyb2	-0.5	-0.7	-1.0	0.7	1.4	0.7
Hyb5	-0.4	-1.2	-0.9	0.6	1.3	1.5
BR	-1.1	-2.5	-0.4	0.9	0.4	3.0

Table 5 Maximum in space and time simulated charge densities ($nC.m^{-3}$) for the schemes T78_eq_RAR, BR and the hybrid schemes with different values of the threshold (2 and 5 $m.s^{-1}.km^{-1}$- Hyb2 and Hyb5). Cloud 3

	Max total negative	Max negative (p+s+a)	Max negative (g+h)	Max total positive	Max positive (p+s+a)	Max positive (g+h)
T78_eq_RAR	-0.5	-0.5	-0.9	0.8	1.2	0.7
Hyb2	-0.5	-0.7	-0.9	0.8	1.3	0.8
Hyb5	-0.3	-0.7	-0.8	0.6	1.2	0.7
BR	-0.3	-1.5	-0.4	0.5	0.4	2.0

The calculation of the Poisson equation is computationally expensive, so the electric potential and the field intensity are calculated only for Cloud 3. The temporal evolution of the maximum electric field in Cloud 3 is shown on Fig. 5. The simulations employing the schemes T78_eq_RAR, Hyb2 and BR produce a lightning between 17:36 and 17:42 MDT at an altitude of 10.6 km AGL, while the field in the Hyb5 simulation reaches only 50 kV.m^{-1}, which is 20% less than the others.

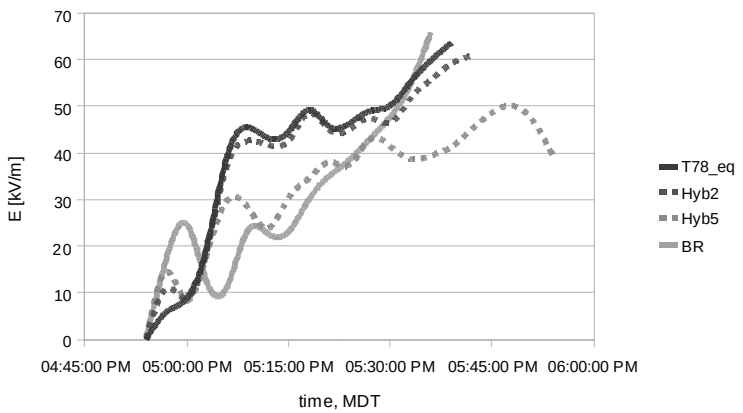

Fig. 5. Temporal evolution of the maximum electric field intensity in Cloud 3

Conclusions

The electric schemes produce both positively and negatively charged graupel and ice crystals and the order of magnitude is realistic, but none of them succeeds to reproduce the observed values.

The comparison between model results and observations can be summarized in the following way:

1. The real storm had a positive dipole structure. This is successfully reproduced by the schemes T78_eq_RAR and Hyb2, but not by BR and Hyb5.

2. Data indicates that negative charge was mainly carried by graupel and positive charge – by pristine ice. The simulations employing the schemes of T78_eq_RAR and Hyb2 are in agreement with these measurements, while BR and Hyb5 are not.

3. All simulations produce electric field of realistic magnitudes and all, except Hyb5, produce a lightning.

The results, presented here, are only the first test for the ability of the new scheme to reproduce the charge structure of the real clouds. These results indicate that the main assumption, on which the new hybrid scheme is based, is adequate. Based on the results presented here, we would recommend a value of 2 [m.s^{-1}.km^{-1}] as an appropriate threshold.

Nevertheless, if we want to come to firm conclusions, thunderstorms with various dynamical and microphysical characteristics have to be simulated. An inductive charging

and lightning discharge parameterizations have to be developed in order to complete the scheme.

Acknowledgments. The authors would like to acknowledge Dr. Orit Altaraz and Prof. Zev Levin from the University of Tel Aviv. Gratitude is also due to the Science Foundation of Sofia University project № 153/2009 and European Social Fund project № BG051PO001-3.3.04-33 / 28. 08. 2009

References

Altaratz O., T. Reisin and Z. Levin, 2005. Simulation of the electrification of winter thunderclouds using the three- dimensional Regional Atmospheric Modeling System (RAMS) model: Single cloud simulations. *J. Geophys. Res.*, 110, D20205, doi:10.1029/2004JD005616.

Barthe C., M. Gilles and J.P. Pinty, 2005. Description and first results of an explicit electrical scheme in a 3D cloud resolving model. *Atm. Res.*, 76, 95-113.

Brooks I.M., C.P.R. Saunders, R.P. Mitzeva and P.L. Peck, 1997. The effect on thunderstorm charging of the rate of rime accretion by graupel. *Atmos. Res.*, 43, 277–295

Cotton W, et al., 2003. RAMS 2001: Current status and future directions. *Meteorol. Atmos. Phys.*, 82, 5–29

Dye J.E., J.J. Jones, W.P. Winn, T.A. Ceri, B. Gardiner, D. Lamb, R.L. Pitter, J. Hallett and C.P.R. Saunders, 1986. Early electrification and precipitation development in a small isolated Montana cumulonimbus. *J. Geophys. Res.*, 91, pp. 1231–1247.

Gardiner B., D. Lamb, R.L. Pitter, J. Hallett and C.P.R. Saunders, 1985. Measurements of Initial Potential Gradient and Particle Charges in a Montana Summer Thunderstorm. *J. Geophys. Res.*, 90(D4), 6079–6086.

Helsdon J.H. Jr and R.D. Farley, 1987. A numerical modeling study of a Montana thunderstorm. *J. Geophys. Res.*, 92(D5), 5645-5659.

Helsdon J.H. Jr, W.A. Wojcik and R.D. Farley, 2001. An examination of thunderstorm-charging mechanisms using a two-dimensional storm electrification model. *J. Geophys. Res.*, 106(D1), 1165–1192.

Jayaratne E.R., C.P.R. Saunders and J. Hallett, 1983. Laboratory studies of the charging of soft-hail during ice crystal interactions. *Q. J. R. Meteorol. Soc.*, 109, 609-630

MacGorman D. and W. Rust, 1998. *The Electrical Nature of Storms.* Oxford University Press, 422 pp.

Mansell E.R. and D.R. MacGorman, C.L. Ziegler, J.M. Straka, 2005. Charge structure and lightning sensitivity in a simulated multicell thunderstorm. *J. Geophys. Res.*, 110, D12101, doi:10.1029/2004JD005287.

Marshall T.C., M.P. McCarthy and W.D. Rust, 1995. Electric field magnitudes and lightning initiation in thunderstorms, *J. Geophys. Res.*, 100(D4), 7097–7103.

Meyers M., R. Walko, J. Harrington and W. Cotton, 1997. New RAMS cloud microphysics parametrization. Part II: The two-moment scheme. *Atmospheric Research*, 45, 3-39

Norville K., M. Baker and J. Latham, 1991. A Numerical Study of Thunderstorm Electrification: Model Development and Case Study, *J. Geophys. Res.*, 96(D4), 7463–7481.

Pereyra R.G., E.E. Avila, N.E. Castellano and C.P.R. Saunders, 2000. A laboratory study of graupel charging. *J. Geophys. Res.*, 105, 20803–20812.

Pielke R.A., W. Cotton, R. Walko, et al., 1992. A Comprehensive Meteorological Modeling System RAMS. *Meteorol. Atmos. Phys.*, 49, 69-91

Saunders C.P.R., W.D. Keith and R.P. Mitzeva, 1991. The Effect of Liquid Water on Thunderstorm charging. *J. Geophys. Res.*, 96(D6), 11,007–11,017.

Saunders C.P.R., H. Bax-Norman, E.E. Avila and N.E. Castellano, 2004. A laboratory study of the influence of ice crystal growth conditions on subsequent charge transfer in thunderstorm electrification. *Quart. J. Roy. Met. Soc.*, 130, 1395-1406.

RAMS Technical Manual (draft) http://www.atmet.com/html/docs/rams/rams_techman.pdf Accessed 12 October 2010

Takahashi T., 1978. Riming electrification as a charge generation mechanism in thunderstorms. *J. Atmos. Sci.*, 35, 1536–1548.

Takahashi T., 1999. Reversal of the sign of the charge on graupel during riming electrification: Measurements in Hokuriku winter clouds and in a wind tunnel. Proc. 11th Intl. Conf. on Atmos. Elect., NASA/CP-1999209261, ed. H. Christian, NASA/ Marshall Space Flight Center, Huntsville, AL, 304-307

Tsenova B. and R. Mitzeva, 2009. New parameterization of non-inductive charge transfer based on previous laboratory experiments. *Atmos. Res.*, 91, 79-86.

Walko R.L., W.R. Cotton, M.P. Meyers and J.Y. Harrington, 1995. New RAMS cloud microphysics parameterization. Part I: The single-moment scheme. *Atmos. Res.*, 38, 29–62.

Appendix

Equations from Brooks et al. (1997), used for the parameterization BR:

Critical RAR:

$T \geq -10.7$: $CRAR = 0.66$

$-10.7 > T \geq -23.8$: $CRAR = -1.47 + 0.2(-T)$

$T < -23.8$: $CRAR = 3.3$

Charge:

$T > -16$:

- $0.078 < RAR < 0.42$: $q = -104.8 \cdot RAR + 7.9$
- $0.42 < RAR < 0.66$: $q = -139.8 \cdot RAR + 92.6$
- $0.66 < RAR < CRAR$: $q = 3.02 - 10.59 \cdot RAR + 2.95 \cdot RAR^2$
- $0.66 < RAR \quad and \quad RAR > CRAR$: $q = 6.74 \cdot RAR - 1.36 \cdot (-T) + 10.5$

$-16 \geq T > -20$:

- $RAR < CRAR$: $q = 3.02 - 10.59 \cdot RAR + 2.95 \cdot RAR^2$
- $RAR > CRAR$: $q = 6.74 \cdot RAR - 1.36 \cdot (-T) + 10.5$

$-20 \geq T$

- $0.18 \leq RAR < 0.36$: $q = 680.6 \cdot RAR - 128.7$
- $0.36 \leq RAR < 0.48$: $q = -966.7 \cdot RAR + 462.9$
- $0.48 \leq RAR$:

$-20 \geq T \geq -23.8$:

- $RAR > CRAR$: $q = 6.74 \cdot RAR - 1.36 \cdot (-T) + 10.5$
- $RAR < CRAR$: $q = 3.02 - 10.59 \cdot RAR + 2.95 \cdot RAR^2$

$-23.8 \geq T$:

$0.48 < RAR < CRAR$: $q = 3.02 - 10.59 \cdot RAR + 2.95 \cdot RAR^2$

$RAR > CRAR$: $q = 6.74 \cdot RAR - 1.36 \cdot (-T) + 10.5$

Equations from Tsenova and Mitzeva (2009) based on the experimental dataset of Takahashi (1978) and presented as a function of RAR - used for the parameterization T78_eq_RAR:

$T > -10$:

$RAR \leq 12.8$:

$$q = 18.37 \cdot RAR - 1.82 \cdot RAR^2 + 0.06 \cdot RAR^3 - 0.004 \cdot T^3 \cdot RAR - 2.581 \cdot T - 0.0004 \cdot T^3 \cdot RAR^3 + 0.006 \cdot T^3 \cdot RAR^2 + 0.15 \cdot T^2 + 0.006 \cdot T \cdot RAR^3 - 0.53 \cdot T \cdot RAR - 8.5059$$

$RAR > 12.8$:

$$q = 4.17952 \cdot T - 0.00007 \cdot T^2 \cdot RAR^2 + 0.01 \cdot RAR^2 - 0.17 \cdot T \cdot RAR - 0.93 \cdot RAR + 0.002 \cdot T \cdot RAR^2 + 0.000001 \cdot T^2 \cdot RAR^3 - 0.00007 \cdot RAR^3 + 50.84454$$

$T \leq -10$:

$RAR \leq 3.2$:

$$q = -3.3515 \cdot T + 1.5 \cdot T \cdot RAR^2 + 63.98 \cdot RAR + 0.03 \cdot T^2 \cdot RAR^3 - 0.0007 \cdot T^3 + 2.57 \cdot T \cdot RAR + 0.02 \cdot T^2 \cdot RAR + 0.001 \cdot T^3 \cdot RAR^3 - 0.002 \cdot T^3 \cdot RAR^2 + 0.13 \cdot T \cdot RAR^3 - 0.1066 \cdot T^2 - 24.5715$$

$3.2 < RAR \leq 25.6$:

$$q = -0.2 \cdot T \cdot RAR + 0.0005 \cdot T \cdot RAR^3 + 0.0112 \cdot T^3 + 19.1993 \cdot T + 0.8051 \cdot T^2 + 0.01 \cdot RAR^3 - 10.42 \cdot RAR + 0.24 \cdot RAR^2 + 167.9278$$

$RAR > 25.6$:

$$q = 4.212661 \cdot T - 0.1 \cdot T \cdot RAR + 0.001 \cdot T \cdot RAR^2 + 0.0005 \cdot T^2 \cdot RAR + 40.96417$$

Нова схема за неиндуктивно наелекризиране на гръмотевичните облаци в атмосферния модел RAMS

А. Брандийска, Р. Мицева, Б. Ценова

Резюме: Разработена е нова схема за неиндуктивно наелектризиране на гръмотевични облаци. Схемата е включена в микрофизичната схема на модела RAMS v.6.0. Механизмът за генериране на заряд използва подхода на Brooks et al., (1997) използвайки скоростта на натрупване на слана (rime accretion rate - RAR). Схемата

съдържа две различни параметризации, базирани на лабораторните експерименти на Takahashi (1978) and Saunders et al. (1991). В модела е включена нов тип хибридна параметризация, която се базира на предположението, че експериментите на Saunders et al. (1991) за валидни за райони със слабо смесване, а експериментите на Takahashi (1978) – за райони със силно смесване. Проведени са моделни симулации на типичен летен гръмотевичен облак (CCOPE, 19 July 1981) и резултатите показват, че предложената хибридна схема е способна да възпроизведе основните характеристики на измереното разпределение на заряда в облака.